



HAL
open science

Auto-activated Electromagnetic Shield Upon High Intensity Radiated Field Illumination

Quentin Tricas, Xavier Castel, Claire Le Paven, Thomas Eudes, Patrice Foutrel, Jérôme Sol, Philippe Besnier

► **To cite this version:**

Quentin Tricas, Xavier Castel, Claire Le Paven, Thomas Eudes, Patrice Foutrel, et al.. Auto-activated Electromagnetic Shield Upon High Intensity Radiated Field Illumination. International Symposium on Electromagnetic Compatibility (EMC Europe), Sep 2022, Gothenburg, Sweden. 10.1109/EM-CEUROPE51680.2022.9901144 . hal-03884530

HAL Id: hal-03884530

<https://hal.science/hal-03884530>

Submitted on 5 Dec 2022

HAL is a multi-disciplinary open access archive for the deposit and dissemination of scientific research documents, whether they are published or not. The documents may come from teaching and research institutions in France or abroad, or from public or private research centers.

L'archive ouverte pluridisciplinaire **HAL**, est destinée au dépôt et à la diffusion de documents scientifiques de niveau recherche, publiés ou non, émanant des établissements d'enseignement et de recherche français ou étrangers, des laboratoires publics ou privés.

Auto-activated Electromagnetic Shield Upon High Intensity Radiated Field Illumination

Quentin Tricas

Safran Electronics & Defense
Univ Rennes, CNRS, IETR - UMR 6164
F-22000 Saint-Brieuc, France
quentin.tricas@univ-rennes1.fr

Thomas Eudes, Patrice Foutrel

Safran Electronics & Defense
Direction de l'Ingénierie Electronique
F-95610 Eragny, France
thomas.eudes, patrice.foutrel@safrangroup.com

Xavier Castel, Claire Le Paven

Univ Rennes, CNRS
IETR - UMR 6164
F-22000 Saint-Brieuc, France
xavier.castel, claire.lepaven@univ-rennes1.fr

Jérôme Sol, Philippe Besnier

Univ Rennes, INSA Rennes, CNRS
IETR - UMR 6164
F-35000 Rennes, France
jerome.sol, philippe.besnier@insa-rennes.fr

Abstract—This paper concerns the protection of electro-optic and electromagnetic sensors embedded into a metallic cavity equipped with a window made of a non-electrically conducting material and optically transparent over the visible light and/or infra-red spectrum. In the presence of high intensity radiated fields, the cavity must be appropriately shielded to protect those sensors, this protection being detrimental to EM sensors sensitivity in their absence. We propose here an automatic and quasi-instantaneous activation of an electromagnetic shield printed on the window glass through the detection of the impinging electromagnetic field. The presented solution is based on thin micrometric mesh-metal film deposited on a glass substrate surrounded by a parallel arrangement of p-i-n diodes polarized by the EM field source itself. An experimental validation is performed using a reverberation chamber to generate the electromagnetic field stress while performing a shielding effectiveness measurement using the nested reverberation chamber test setup.

Index Terms—Electromagnetic shielding, high-intensity radiated fields (HIRFs), micrometric mesh metal film, optical transparency, p-i-n diode, reverberation chamber, shielding effectiveness.

I. INTRODUCTION

High Intensity radiated fields (HIRFs) applied to optical and/or electromagnetic (EM) sensors can be very detrimental, creating issues such as performance and data loss, hacking or data corruption, and even partial or total destruction of the sensors in the most extreme cases [1], [2], [3], [4]. Conventional solutions to protect electronic equipment against HIRFs imply the use of metallic housing to form a Faraday cage. However, in case of optical sensors, the Faraday cage must handle an interface window exhibiting high optical transparency over the entire operational spectrum of the above sensors. Such a window is detrimental to the shielding effectiveness (SE) of the housing. Multiple technical solutions fulfilling both electromagnetic shielding at radio frequencies and optical transparency have been published over the years [5]. Among them, micrometric mesh metal films offer significant shielding

performance and are easily adapted to the targeted radiofrequency range [6], [7], [8].

This solution can indeed provide high SE over a very large frequency range up to dozens of GHz, while maintaining a high level of optical transparency (higher than 80%) over the entire visible or infrared range. In a recent contribution [9], the authors have presented a solution made of a micrometric mesh-metal film screen whose SE level is controlled through the adjustment of the contact impedance between the screen and its electrically conducting support. This impedance adjustment was ensured by the bias current variation of a set of peripheral p-i-n diodes. In this communication, the concept is extended to design an auto-activated shield for which the HIRF source itself triggers the p-i-n diodes polarization in order to protect the electro-optic equipment. It is based on sensing the radiated electromagnetic field and shaping the induced signal. An experiment performed in a reverberation chamber (RC) sheds some light on the concept feasibility, using the RC simultaneously as the source of electromagnetic field to be protected against, and as a SE measurement setup.

This paper is organized as follows. In section II, the principle of the p-i-n diode activated electromagnetic screen is briefly recalled. Section III deals with the presentation of the electronic circuit used to shape the electromagnetically induced signal by the source of electromagnetic radiation. The dedicated experimental setup and associated results are provided in section IV, before concluding.

II. THE P-I-N DIODE ACTIVATED ELECTROMAGNETIC SCREEN

As a starting point, the variation of the SE may be obtained through the modification of the contact impedance between the shielding screen and its electrically conducting support. More precisely, the intrinsic SE performance of the stand-alone screen is attainable only if the contact impedance is significantly lower than the screen impedance.

In [10], this was investigated through the examination of the SE of a metallic sample placed into a metallic sample-holder with or without electrical continuity. The shielding efficiency was studied for different contact configurations between the sample and its support. Between 1 GHz and 40 GHz, it was shown that SE level dropped from the 60 - 80 dB range to about 10 - 40 dB one when going from virtually perfect electrical contact towards no electrical continuity at all.

In [6], the SE variation of optically transparent films was made possible by just changing the edge geometry of the screen. The electrical contact between the periphery of the micrometric mesh metal screen and its housing was provided by a set of regularly spaced and thin metal ribbons. The variation of the number of contact ribbons was proved to significantly modify the screen SE performance while keeping the meshed part of the screen identical, especially its optical transparency. The fabricated samples showed a SE variation up to 35 dB at 2 GHz and 15 dB at 18 GHz according to the nested RC measurement principle (see Fig. 14 in [6]).

Recently, the authors presented an important advance of this early proposal, using a set of p-i-n diodes to perform an automatic, controlled and reversible change of the contact impedance of each connecting ribbon. The bias of all p-i-n diodes was controlled simultaneously from a DC voltage/current source [9]. We briefly recall its principle and properties.

The sample in [9] consisted of a 50 mm square sample of 0.7 mm-thick soda-lime glass (Fig. 1) partly covered (using radiofrequency sputtering technique followed by photolithography and wet etching processes) by a thin metal layer (2 μm -thick silver layer onto a 5-nm-thick titanium underlayer) arranged in four different parts:

- The first and main one consisted of a square micrometric mesh silver/titanium layer located in the center of the shield. It is composed of 10 μm -width metal strips periodically spaced by 200 μm mesh pitch. This central part exhibits a measured optical transparency equal to 84% in the visible light spectrum
- The second part consists of a 0.5 mm-width silver/titanium strip surrounding the central micrometric mesh metal area.
- The third part is made of a 4.8 mm-width silver/titanium strip that covers the external periphery of the screen. It ensures a strong electrical contact between the sample and the Faraday cage used in the experimental part of the study (see section IV).
- Finally, these last two metal areas are separated by a 2 mm-width slot filled by a hundred and thirty-two 0.304 mm-width metal ribbons, 0.792 mm-spaced on the four sides of the sample. A 8.2 Ω SMD resistor (reference YAG6435CT-ND from Yageo) and a p-i-n diode (reference MA4AGFCP910 from MACOM) are implemented in series on each metal ribbon (Fig. 2).

In addition, a 1.3 mm-side metal square is located in the lower left corner of the screen to allow the direct current (DC)

supply from an external power source to feed the p-i-n diodes through the yellow wire seen in Fig. 1.

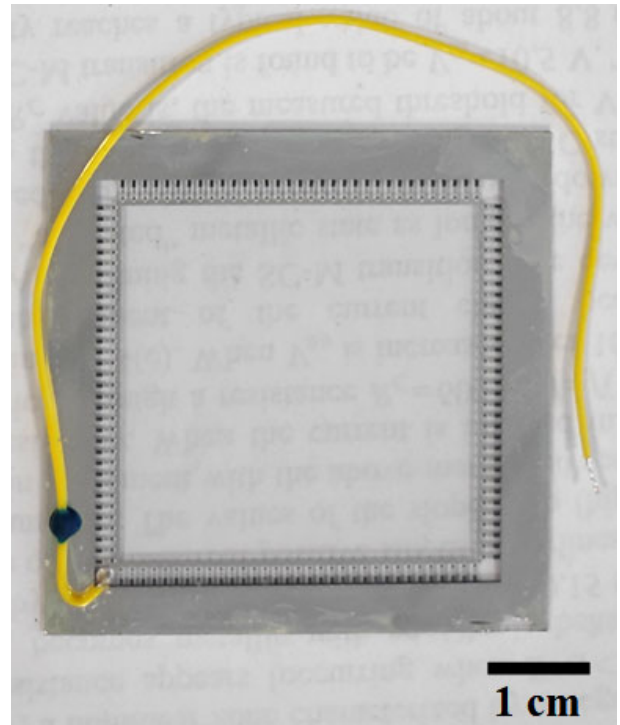


Fig. 1. Optically transparent screen made of the mesh metal film deposited on 50 mm \times 50 mm \times 0.7 mm soda-lime glass substrate. The central micrometric mesh silver/titanium area exhibits a measured optical transparency equal to 84% in the visible light spectrum

III. THE DETECTOR CIRCUIT

Due to the fast switching time of the p-i-n diodes, the SE level of the screen may vary very fast and significantly if the diodes bias is changed from forward to reverse configuration and reciprocally. Therefore, we hypothesize that the SE level of the screen could be increased when it is exposed to very intense electromagnetic fields (i.e. electromagnetic radiation of the HIRF type) and upon their detection. Under HIRFs, a RF detector could deliver adequate DC currents and voltages to reach a forward bias and supply of p-i-n diodes set. This concept is therefore experimentally investigated in the present communication.

It would be possible to avoid any signal amplification and external supply of energy other than that of the HIRFs themselves. As far as this 132 p-i-n diodes prototype is concerned, a supply of 150 mA under a voltage of 1.4 V would be necessary to reach the complete forward bias. However, it was shown in [9] that 10 mA are enough to reach a significant SE contrast. The assembly would therefore be self-sufficient in energy, in addition to being self-adaptive.

This experimental configuration was not selected here to test this concept, given the difficulty of generating HIRFs in the laboratory in the targeted frequency band. We therefore opted for detecting the electromagnetic field radiation and

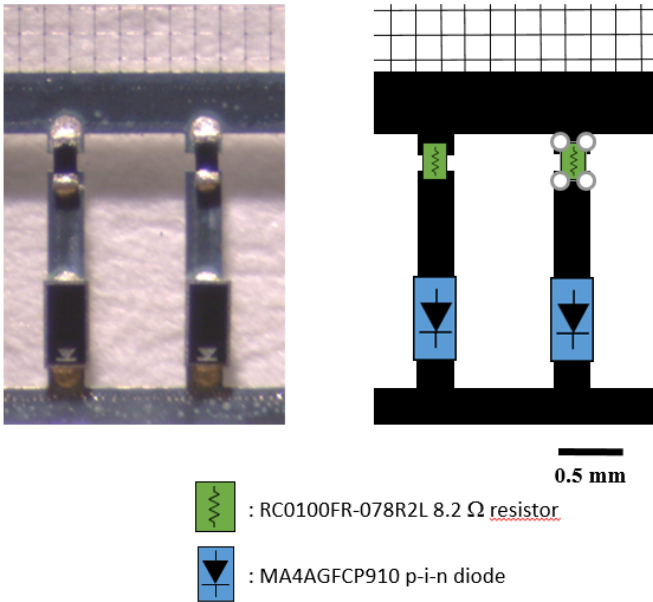


Fig. 2. Photograph and schematic of the series resistances and p-i-n diodes implemented on each metal ribbon and located between micrometric mesh metal area and the external periphery of the screen

then shape it with an adequate amplification chain requiring an external source of energy. Also, this made it possible to activate the shielding screen with a lower electromagnetic field stress, while enabling a SE measurement using a vector network analyser (VNA). Therefore, in the following, the auto-activated increase of SE is achieved using the electromagnetic field radiated by an antenna supplied by the RF power source of a VNA (at a maximum RF power of 16 dBm) in a RC.

The detection and amplification circuit is depicted schematically in Fig. 3. Its amplifier stages are implemented on a test-board shown in Fig. 4, the output being connected to the screen. For measurements in section IV, the input stage of the detection and amplification circuit is connected to a receiving antenna. The input stage consists of a low-noise amplifier LNA Miteq AFS4-00101200-22-10P-4. The gain of this LNA is approximately 26 dB in the 100 MHz – 12 GHz range and is supplied by a 15 V DC power supply. The output of the LNA is then routed to the input of a Keysight 33330C RF (Schottky diode) detector. This detector produces a DC output voltage of 0.5 mV per μ W of received RF power in the 10 MHz to 18 GHz frequency range. The output of the detector is then connected to the input of a TLE2144ACN operational amplifier, integrated in a non-inverting configuration, allowing for the DC voltage to be amplified at its output. This voltage amplifier is followed by a current amplifier based on a KSP 2222A NPN bipolar transistor. It allows current amplification to reach at least a few dozens of mA up to 150 mA at its output to ensure switching of the p-i-n diodes into their conducting state. Both amplifiers are powered by a 9 V battery.

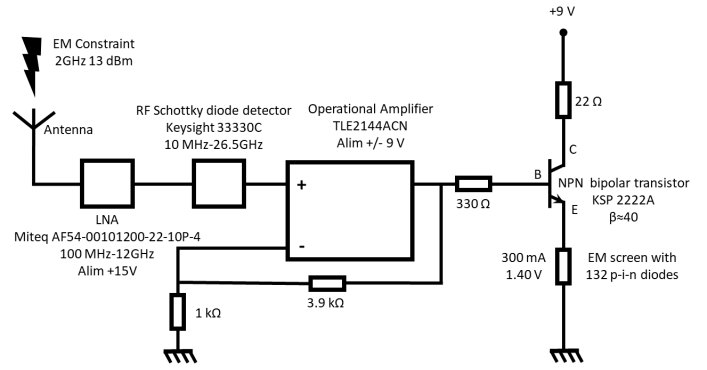


Fig. 3. The detector circuit composed of a low-noise amplifier, a Schottky diode detector, an op-amp voltage amplifier and a bipolar transistor current amplifier

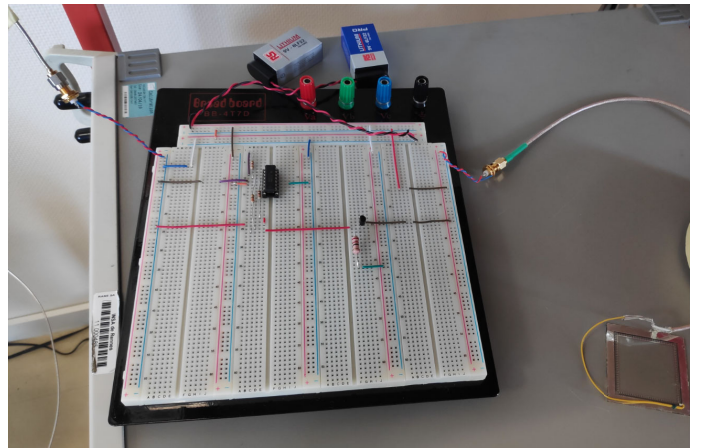


Fig. 4. View of the board for DC signal amplification placed within the Faraday cage

IV. EXPERIMENTAL RESULTS

The experimental setup is presented in Fig. 5. The amplification stages of the detector and amplification circuit (i.e. the board in Fig. 4) are placed into a small Faraday cage placed itself in a large RC. This setup allows for the measurement of SE according to the nested RC chamber method, following the method called "SE3" in [11]. However, to reduce uncertainties in measurements, the RC Q -factor is assumed to be identical for both configurations of SE measurements (in absence or presence of the screen under test). The output of the current amplifier is connected to the yellow wire supplying the p-i-n diodes of the screen installed in the sample-holder of the small Faraday cage. The input of the voltage amplifier is connected through an interface panel on a wall of the Faraday cage. It is then connected to the LNA and to a receiving horn antenna (see Fig. 6). The yellow box lying on the ground and visible in Fig. 5 is the power supply used for the LNA.

The VNA generates a constant wave signal in the 2 - 18 GHz frequency range at its maximum available power (16 dBm). This signal is injected to the input of a horn antenna radiating the electromagnetic field in the RC. Both frequency



Fig. 5. View of the experimental setup installed in the large RC. The Faraday cage is shown with the source antenna on the top and the receiving antenna on its left side. The front size contains the windows where the screen is inserted for SE measurements

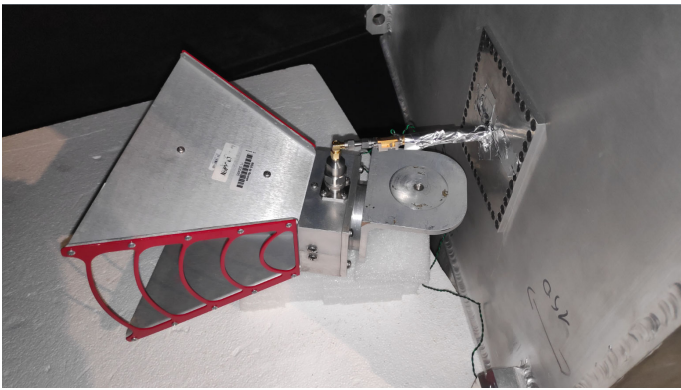


Fig. 6. Detection antenna, low noise amplifier and rectifier outside the Faraday cage

and mechanical stirring are used to perform the SE evaluation. Preliminary tests have shown that the current measured at the output of the bipolar transistor reaches 300 mA under 1.4 V when the whole device is placed in the RC, for a power generated by the VNA of 13 dBm at the frequency of 2 GHz. It is therefore expected that the diodes should be adequately biased, at least in the lower range of the tested frequency band since the effective area of the receiving antenna decreases with the square of the frequency.

The radiated field in the RC with a 16 dBm source was assessed from the Q-factor evaluation performed in the current measurement configuration. The assessed average electric-field strength is plotted in Fig. 7 whereas the power recorded by the receiving horn antenna is plotted in Fig. 8. The average electric-field strength lies between 14 V/m at 2 GHz and 10 V/m at 18 GHz and the corresponding assessment of the received power at the receiving antenna shows that it is significant in the lower frequency range and evaluated at 0.3 mW at 2 GHz down to 0.05 mW at 6 GHz and 0.01 mW at 10 GHz. In the higher frequency range, the induced power appears to be too small to reach the forward bias. At 2 GHz, 6 GHz and 10 GHz, the output DC voltage at the output of the

detector is assessed to be 3 V, 0.5 V and 0.1 V respectively. Despite amplification, we predict that the p-i-n diodes might be not polarized beyond 10 GHz using this circuit.

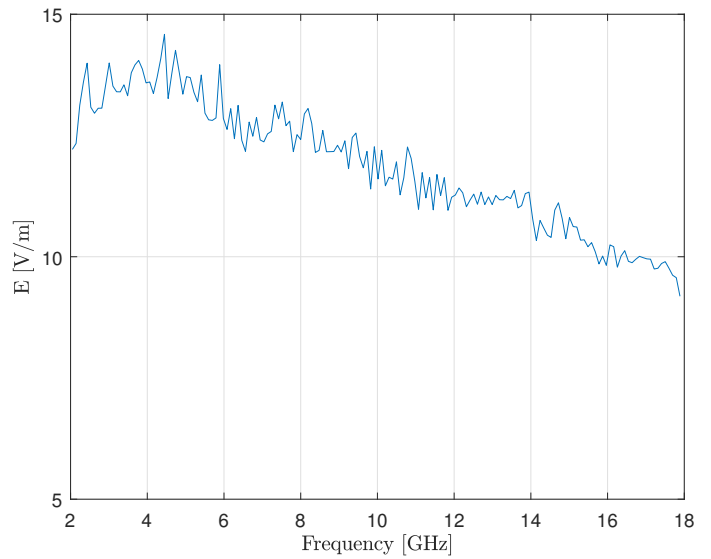


Fig. 7. Average electric-field in the RC assessed from Q-factor measurement connecting the transmitting horn antenna to VNA supplied with a 16 dBm internal RF power source

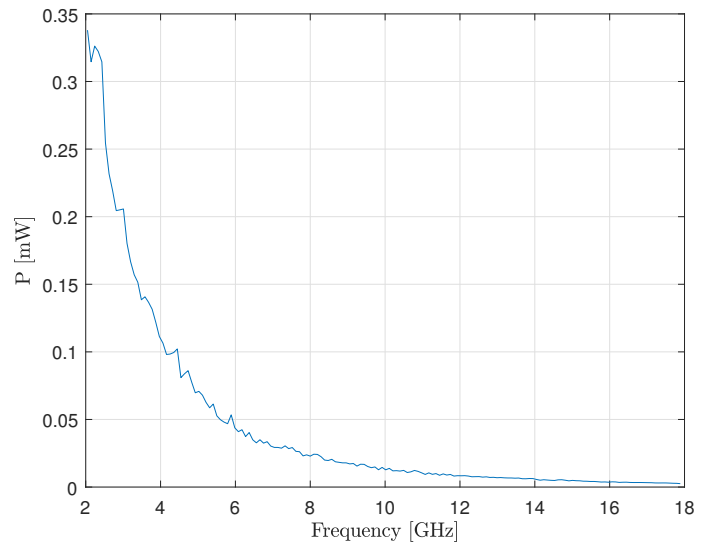


Fig. 8. Average received power at the receiving antenna calculated from the average electric-field in the RC plotted in Fig. 7

The SE results are shown in Fig. 9. The red curve corresponds to the SE level as measured in the conditions detailed above. A second measurement was carried out in the same conditions but after disconnection of the receiving antenna (black curve).

First, the difference observed between the two curves clearly shows that the signal picked up by the receiving antenna and transformed through the detection and amplification circuit made it possible to dynamically modify the SE of the shielding

screen. This corresponds to a self-adaptation in the presence of the electromagnetic field radiated in the RC.

Second, we observe that the SE variation is restricted to the lower part of the frequency range and is also limited in magnitude, compared with SE variation as measured in [9]. The effect was predictable and mainly due to the decrease of the effective area of the receiving antenna. This is in line with the decrease of the received power observed in Fig. 8.

These results validate the concept of an auto-activated screen upon detection of an electromagnetic field radiation to be protected from. In this specific conditions, the circuit detects and induces a forward bias of the diodes for a rather low intensity radiated field (of about 10 V/m) in the 2-8 GHz range. It is therefore applicable to higher field strengths of several hundred V/m, adapting the detection circuit proposed here as a demonstrator.

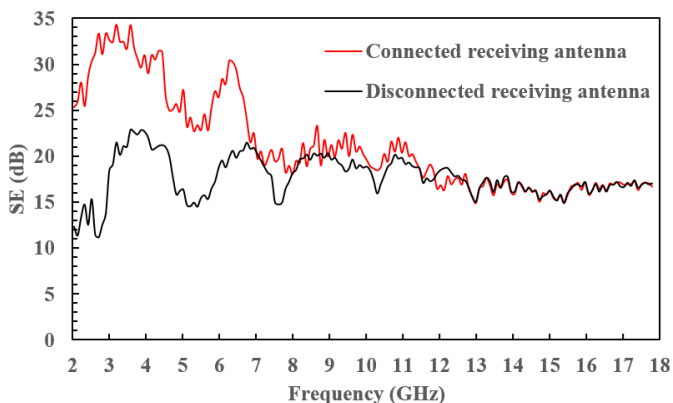


Fig. 9. Measurement of the shielding screen SE using the detection and amplification circuit. The receiving antenna is connected (red curve) and disconnected (black curve) from the input of this circuit to highlight the increase level of SE provided by the forward bias of the diodes

V. CONCLUSION

In some situations, electromagnetic and electro-optic sensors must be adequately protected against HIRFs. However, in absence of any significant electromagnetic perturbation, permanently high SE limits the sensitivity of electromagnetic sensors. A self-adapting device adjusting the SE level of optically transparent shielding screen is therefore relevant. In this paper, we have proposed an automatic, , controlled, reversible and quasi-instantaneous (typically a few microseconds according to the detector circuit and p-i-n diodes properties) activation of a shielding screen printed on a window glass through the detection of the impinging electromagnetic field. This is achieved through the sensing of the illuminating electromagnetic source and the shaping of the captured signal. The resulting DC signal polarizes a set of p-i-n diodes surrounding the optically transparent shielding screen to lower the contact impedance between the screen and its housing. An experiment carried out at a rather low intensity radiated field in RC, thus requiring an active electronic circuit, highlighted the feasibility of such a solution.

ACKNOWLEDGMENT

The authors warmly acknowledge Thomas Batté from NanoRennes, Jean-Claude Magnard and Laurent Delarbre from SAFRAN Electronics & Defense at Valence, for the SMD implementation on the shielding screens.

This work was supported in part by SAFRAN Electronics & Defense under Grant 2018/1107, in part by the European Union through the European Regional Development Fund, in part by the Ministry of Higher Education and Research, in part by the Région Bretagne, and in part by the Département des Côtes d'Armor and Saint-Brieuc Armor Agglomération, through the CPER Projects 2015-2020 MATECOM and SOPHIE/STIC & Ondes.

REFERENCES

- [1] M. G. Backstrom and K. G. Lovstrand, "Susceptibility of electronic systems to high-power microwaves: summary of test experience," *IEEE Trans. Electromagn. Compat.*, vol. 46, no. 3, pp. 396–403, Aug. 2004. doi: 10.1109/TEMC.2004.831814.
- [2] D. Nitsch, M. Camp, F. Sabath, J. L. Ter Haseborg, and H. Garbe, "Susceptibility of some electronic equipment to HPEM threats," *IEEE Trans. Electromagn. Compat.*, vol. 46, no. 3, pp. 380–389, Aug. 2004. doi: 10.1109/TEMC.2004.831814.
- [3] D. F. Kune et al., "Ghost talk: mitigating EMI signal injection attacks against analog sensors," in *Proc. IEEE Symp. Secur. Priv.*, Berkeley, CA, USA, 2013, pp. 145–159. doi: 10.1109/SP.2013.20. doi: 10.1109/SP40000.2020.00001.
- [4] Y. Zhang and K. Rasmussen, "Detection of electromagnetic interference attacks on sensor systems," in *Proc. IEEE Symp. Secur. Priv.*, San Francisco, CA, USA, 2020, pp. 203–216.
- [5] B. Ray, S. Parmar, and S. Datar, "Flexible and transparent EMI shielding materials," in *Adv. Mater. Electromagn. Shield.*, John Wiley & Sons, Ltd, Hoboken, NJ, USA, 2018, pp. 167–175.
- [6] M. Croizer, Q. Tricas, P. Besnier, X. Castel, and P. Foutrel, "Control of shielding effectiveness of optically transparent films by modification of the edge termination geometry," *IEEE Trans. Electromagn. Compat.*, vol. 62, no. 6, pp. 2431–2440, Dec. 2020. doi: 10.1109/TEMC.2020.2982644
- [7] P. D. Tung and C. W. Jung, "High optical visibility and shielding effectiveness metal mesh film for microwave oven application," *IEEE Trans. Electromagn. Compat.*, vol. 62, no. 4, pp. 1076–1081, Aug. 2020. doi: 10.1109/TEMC.2019.2927923
- [8] Z. Jiang et al., "Ultrathin, lightweight, and freestanding metallic mesh for transparent electromagnetic interference shielding," *Opt. Express*, vol. 27, no. 17, pp. 24194–24206, Aug. 2019. doi: 10.1364/OE.27.024194
- [9] Q. Tricas, X. Castel, P. Besnier, C. Le Paven, P. Foutrel, "Dynamic control of the shielding effectiveness of optically transparent Screens," *IEEE Trans. Electromagn. Compat.*, pp. 1–7 (early access). doi: 10.1109/TEMC.2022.3146245
- [10] J. Catrysse, T. Grenson, F. Vanhee, D. Pissort, C. Brull, "The importance of continuous gasket conductivity up to 40 GHz," 2013 in *Proc. Int. Symp. Electromagn. Compat.*, EMC Europe, Brugge, Belgium, 2013, pp. 536–540.
- [11] C. L. Holloway, D. A. Hill, J. Ladbury, G. Koepke, and R. Garzia, "Shielding effectiveness measurements of materials using nested reverberation chambers," *IEEE Trans. Electromagn. Compat.*, vol. 45, no. 2, pp. 350–356 May 2003. doi: 10.1109/TEMC.2003.809117